Dynamics of tetrahydrofuran as minority component in a mixture with poly(2-(dimethylamino)ethyl methacrylate): a neutron scattering and dielectric spectroscopy investigation

G. Goracci,[1, a)] A. Arbe,[1] A. Alegría,[1, 2] W. Lohstroh,[3] Y. Su,[4] and J. Colmenero[1, 2, 5]

[1)] *Centro de Física de Materiales (CFM) (CSIC–UPV/EHU) – Materials Physics Center (MPC), Paseo Manuel de Lardizabal 5, 20018 San Sebastián, Spain*

[2)] *Departamento de Física de Materiales (UPV/EHU), Apartado 1072, 20080 San Sebastián, Spain*

[3)] *Heinz Maier-Leibnitz Zentrum, Technische Universität München, Lichtenbergstraße 1, D-85748 Garching, Germany*

[4)] *Jülich Centre for Neutron Science JCNS, Forschungszentrum Jülich GmbH, Outstation at MLZ, Lichtenbergstraße 1, 85747 Garching, Germany*

[5)] *Donostia International Physics Center, Paseo Manuel de Lardizabal 4, 20018 San Sebastián, Spain*

We have investigated a mixture of poly(2-(dimethylamino)ethyl methacrylate) (PDMAEMA) and tetrahydrofurane (THF) (70wt%PDMAEMA/30wt%THF) by combining dielectric spectroscopy and quasielastic neutron scattering (QENS) on a labelled sample, focusing on the dynamics of the THF molecules. Two independent processes have been identified. The 'fast' one has been qualified as due to an internal motion of the THF ring leading to hydrogen displacements of about 3 Å with rather broadly distributed activation energies. The 'slow' process is characterized by an Arrhenius-like temperature dependence of the characteristic time which persists over more than 9 orders of magnitude in time. The QENS results evidence the confined nature of this process, determining a size of about 8 Å for the volume within which THF hydrogens' motions are restricted. In a complementary way, we have also investigated the structural features of the sample. This study suggests that THF molecules are well dispersed among side-groups nano-domains in the polymer matrix, ruling out a significant presence of clusters of solvent. Such a good dispersion, together with a rich mobility of the local environment, would prevent cooperativity effects to develop for the structural relaxation of solvent molecules, frustrating thereby the emergence of Vogel-Fulcher-like behavior, at least in the whole temperature interval investigated.

[a)]Electronic mail: sckgorag@ehu.es

I. INTRODUCTION

The dynamics in glass formers constitutes a complex problem. These systems display a variety of dynamical processes including the structural or α-relaxation, which freezing leads to the glassy state. Such complexity becomes obviously even more intricate if mixtures are considered. However, mixtures are ubiquitous both in nature as well as constituents of materials designed for practical purposes. The advantage they present is that the material properties can be tailored by varying the composition. Characterizing the dynamical processes in the components of the mixture and understanding the effects of blending on these motions is fundamental from a basic and an applied perspective, as well as a challenging problem from an experimental and a theoretical point of view.

In polymer blends[1–5] , mixtures of oligomers and low-molecular weight systems[6,7] and also in mixtures of polymers and low-molecular weight systems[8–10] it has been shown the existence of two different glass transitions associated to the freezing of the α-relaxation corresponding to each of the components in the system. A particularly interesting situation has been identified for these mixtures when the neat components present a large difference in their glass-transition temperatures. Under this condition, a dynamic asymmetry –ratio between the structural relaxation times of the components in the mixture– is induced, which gradually increases with decreasing temperature and can become extremely high in the vicinity and below the glass-transition of the slowest component. Then, confinement effects are expected on the α-process of the fastest component upon vitrification of the α-relaxation of the slowest component[1] . These effects would manifest in a crossover from a high-temperature regime where the dynamics of the slow component is fast enough to allow the fast component relax in a close to equilibrium situation, toward a low-temperature regime where the slow component imposes a rigid environment to the motions of the fast component, hampering the cooperative processes which would naturally occur in the supercooled liquid regime. A clear signature of the confinement situation is the Arrhenius-like temperature dependence of the characteristic time. Thus, a crossover from Vogel-Fulcher to Arrhenius dependence is expected upon cooling down the system. This crossover was first observed in blends of polystyrene (PS) / poly(vinyl methyl ether) (PVME)[3] . Other investigations in polymer blends [polyethyleneoxide (PEO) /poly(methyl methacrylate) (PMMA)[8,11] , PEO/poly(vinyl acetate) (PVAc)[12] , PEO/PS,[13]] have also reported this phenomenon. We

note that the explanation in terms of a crossover from equilibrium-like situation toward confinement by the surrounding vitrified matrix has also been proposed for the controversial 'strong-fragile' transition reported for confined water in a large number of environments[14] .

In concentrated aqueous solutions the role played by H-bonds might be fundamental to determine the dynamical features. Therefore, considering pairs of components interacting via weaker interactions like van der Waals removes such an important ingredient and might shed light on the general problem of dynamics in dynamically asymmetric mixtures. We note that a simple way to induce a large dynamic asymmetry is to consider a mixture of a low molecular weight material and a polymer. Moreover, this kind of systems –plasticized polymers– are of great interest from an applied viewpoint. Interestingly, a Vogel-Fulcher to Arrhenius crossover has also been recently reported for methyl-tetrahydrofuran (MTHF) as minority component in mixtures with polystyrene[7]. The question whether this is a general phenomenon or under which circumstances it appears is still open.

Here we investigate the molecular dynamics in a mixture of 70wt% poly(dimethylaminoethyl methacrylate) (PDMAEMA) with 30wt% tetrahydrofuran (THF). As mentioned above, this kind of studies constitute a challenge from an experimental point of view, since covering a large dynamic range and selectivity to the different components are required. For this purpose, we have combined broadband dielectric spectroscopy (DS) with quasielastic neutron scattering (QENS) techniques. The former allows exploring a very wide range in frequencies, while the latter offers selectivity to a given component, through isotopic (H/D) labeling –deuteration significantly reduces the scattered intensity, thereby 'hiding' the deuterated component to neutrons. The QENS experiments then are sensitive to the incoherent scattering related to hydrogen self-motions of the protonated component. Not least, QENS also provides space/time resolution at a molecular level through the momentum transfer dependence of the magnitudes measured. In a recent work[15] we have applied this strategy to study the majority polymeric component in this mixture. We characterized the dynamic processes attributable to PDMAEMA in the mixture (α and β-relaxations and methyl groups rotations), and determined the influence of the solvent on these processes by comparison with the results on the dry polymer. Methyl-group dynamics are not affected. On the contrary, the α-relaxation is drastically modified ('plasticization' effect) and one of the two contributions underlying the β-relaxation of the dry polymer, namely the slowest one, is completely suppressed by the presence of THF molecules. In the present complementary

investigation, we focus on the dynamics of the solvent molecules. Thereby a sample consisting of deuterated polymer and protonated THF has been used in the QENS experiments. To provide structural information –crucial to interpret the dynamic results, as we will see– we have also performed diffraction measurements on the dry polymer and the mixture.

We have identified two dynamical processes for THF molecules. The faster one can be related to internal degrees of freedom of the ring. The slower one does not evidence, in the whole range investigated, any signature of a crossover from Vogel Fulcher to Arrhenius behavior upon cooling, but displays the latter in a persistent way. We rationalize the absence of Vogel Fulcher behavior basing us on the good dispersion of the small THF molecules in nano-domains rich in polymeric side groups, where a fast dynamics of the environment would frustrate the development of the THF intermolecular cooperativity.

II. EXPERIMENTAL SECTION

A. Samples

Poly(dimethylaminoethyl methacrylate) in its protonated (PDMAEMA) and deuterated (dPDMAEMA) forms was purchased from Polymer Source. The average molecular weight of PDMAEMA was $M_w = 57000$ g/mol, with polydispersity $M_w/M_n = 3.0$, while for dPDMAEMA $M_w = 80000$ g/mol and $M_w/M_n = 2.0$. To exclude the presence of water or other solvent molecules in the pure polymer, PDMAEMA and dPDMAEMA were annealed for 7 h at 100°C under vacuum. Concentrated mixtures with THF 30%wt (1 molecule of THF/ polymer monomer) were prepared by mixing the dry polymer with the appropriate amounts of THF. Dielectric spectroscopy measurements were performed on samples with PDMAEMA while neutron scattering experiments were carried out on samples with deuterated polymer. The calorimetric glass-transition temperature determined by differential scanning calorimetry (DSC) was 227 K. DSC measurements did not show signs of crystallization.

B. Dielectric Spectroscopy

Broadband dielectric spectrometer Novocontrol Alpha-S and high frequency dielectric spectrometer Agilent E4991A RF-Impedance Analyzer were used to measure the complex

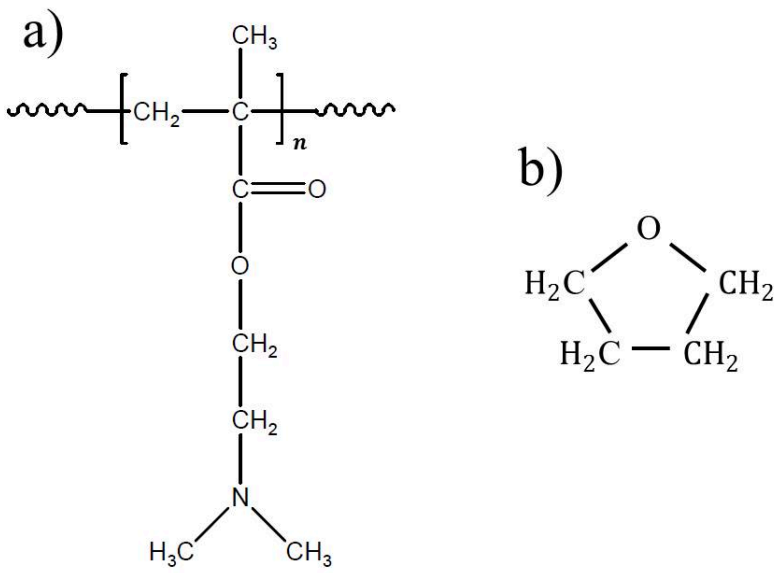

Figure 1. Chemical formulae of PDMAEMA (a) and THF molecule (b).

dielectric function $\epsilon^*(\omega) = \epsilon^{'}(\omega) - i\epsilon^{''}(\omega)$, covering a frequency range of 10^{-2}-10^{9} Hz. PDMAEMA/THF 30%wt was investigated using parallel gold-plated electrodes with a diameter of 20 and 10 mm for low and high frequency measurements respectively. Measurements were carried out under isothermal conditions, from 115 K up to 300 K –in order to avoid a significant solvent evaporation– each 5 K with a temperature stability better than 0.1 K.

C. Neutron Scattering

The intensity recorded in a neutron scattering experiment contains coherent and incoherent contributions. The coherent part is related to relative positions of pairs of atoms and gives information about the structural organization and collective dynamics of the system while the incoherent contribution contains information about single atom dynamics. The incoherent cross-section σ_{inc} of the hydrogen nucleus is overwhelming as compared to the cross-sections (both, coherent and incoherent) of carbon, oxygen, nitrogen and deuterium. Therefore, deuteration of a given component in the system leads to a huge suppression of the contribution of such a component to the scattered intensity. In this way, we can selectively follow the H-self motions of the protonated component in our system. Since we are interested on the THF dynamics in the mixture, the sample investigated was composed by

30wt%THF and 70wt%dPDMAEMA. In order to determine the coherent and incoherent contributions to the scattered intensity, polarization analysis techniques were applied.

1. Diffraction with Polarization Analysis Measurements

Considering that there is no magnetic scattering involved, the magnitudes measured in a diffraction experiment with polarization analysis are the non-spin-flipped (NSF) and the spin-flipped (SF) differential cross sections related to incoherent and coherent differential scattering cross sections by:

$$\left(\frac{d\sigma}{d\Omega}\right)_{SF} = \frac{2}{3}\left(\frac{d\sigma}{d\Omega}\right)_{inc} \tag{1}$$

$$\left(\frac{d\sigma}{d\Omega}\right)_{NSF} = \left(\frac{d\sigma}{d\Omega}\right)_{coh} - \frac{1}{3}\left(\frac{d\sigma}{d\Omega}\right)_{inc} \tag{2}$$

Measurements were carried out by using the diffuse scattering spectrometer DNS (MLZ, Garching, Germany). An incident neutron wavelength of $\lambda = 4.2$ Å was used covering a range in momentum transfer Q from Q=0.2 Å^{-1} to Q=2.67 Å^{-1}. We investigated dPDMAEMA/THF and PDMAEMA/THF mixtures as well as a dry polymer sample at several temperatures below and above the respective glass-transition temperatures. Background correction was done by subtracting the intensity scattered by an empty aluminum sample holder.

2. Quasielastic Neutron Scattering Measurements

The cold neutron time-of-flight spectrometer TOFTOF (MLZ, Garching, Germany) was used to carry out QENS measurements providing information about the dynamics through the energy transfer analysis of the scattered neutrons. Using $\lambda = 7$Å, an energy resolution of 25 μeV was achieved. In the experiment, a flat aluminum sample holder sealed by indium wire was used in order to prevent solvent loss. The thickness of the sample holder was chosen in order to obtain a transmission close to 90%, to neglect possible multiple scattering contributions. Vanadium in a flat aluminum cell was measured at room temperature to correct the detector efficiency after the subtraction of the empty cell signal. The resolution

function was determined measuring the sample at 10 K. dPDMAEMA/THF was investigated at 180, 200, 250 and 270 K.

III. EXPERIMENTAL RESULTS

A. Structure Factors

For the three samples investigated, Figs. 2 and 3 show the DNS results represented as the ratio between the coherent and the incoherent differential cross sections. Since the latter does not contain structural information, the magnitude shown directly reflects the partial structure factor revealed by coherent scattering. In all cases, the pattern shows a peak at $Q \approx 1.3$ Å^{-1}. For the dPDMAEMA/THF sample a strong increase of the coherent signal toward low-Q values is observed, while for the protonated samples a peak centered around ≈ 0.5 Å^{-1} is resolved. The results are hardly temperature dependent.

B. Dielectric Spectroscopy

At temperatures around and above the glass transition of the sample, dielectric spectroscopy results are dominated by a strong conductivity contribution and the α-relaxation of the polymer. Since in this work we are interested in the molecular motions of THF, we will focus our attention on the processes attributable to this component, that are resolvable at lower temperatures. Figures 4(a) and (b) show the dielectric loss of the mixture at different temperatures, obtained by the two instruments used. The results at 125 K have been merged in Fig. 4(c). At this temperature, two main processes –a 'slow' one leading to a maximum at about $f_{max} \approx 1$ Hz and a 'fast' one centered at about $f_{max} \approx 10^8$ Hz– can be well resolved. Between both relaxations, a third one can be envisaged with a much weaker intensity, which produces a kind of shoulder on the high-frequency flank of the 'slow' process. This less prominent relaxation at intermediate frequencies can be attributed, as it was shown in a previous study on the polymer component dynamics[15], to motions contributing to the β-process of the polymer. The other two main relaxations can be assigned to dynamics involving THF molecules[16] .

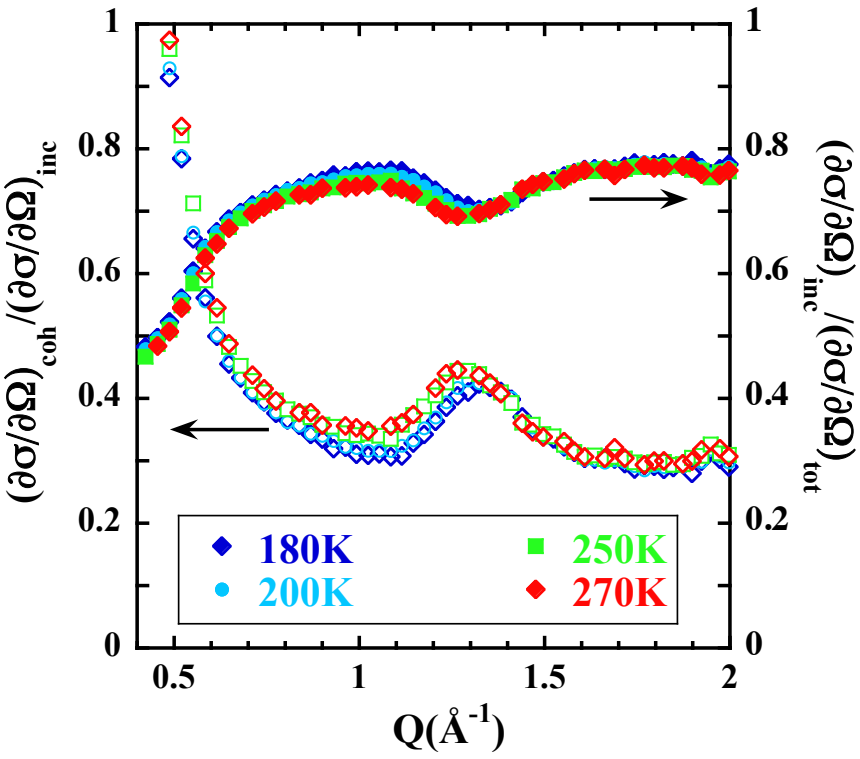

Figure 2. Ratio between the coherent and the incoherent differential scattering cross sections measured by DNS on dPDMAEMA/THF (empty symbols). Filled symbols show the ratio between the incoherent and the total (coherent plus incoherent) differential scattering cross sections. Different symbols correspond to the indicated temperatures.

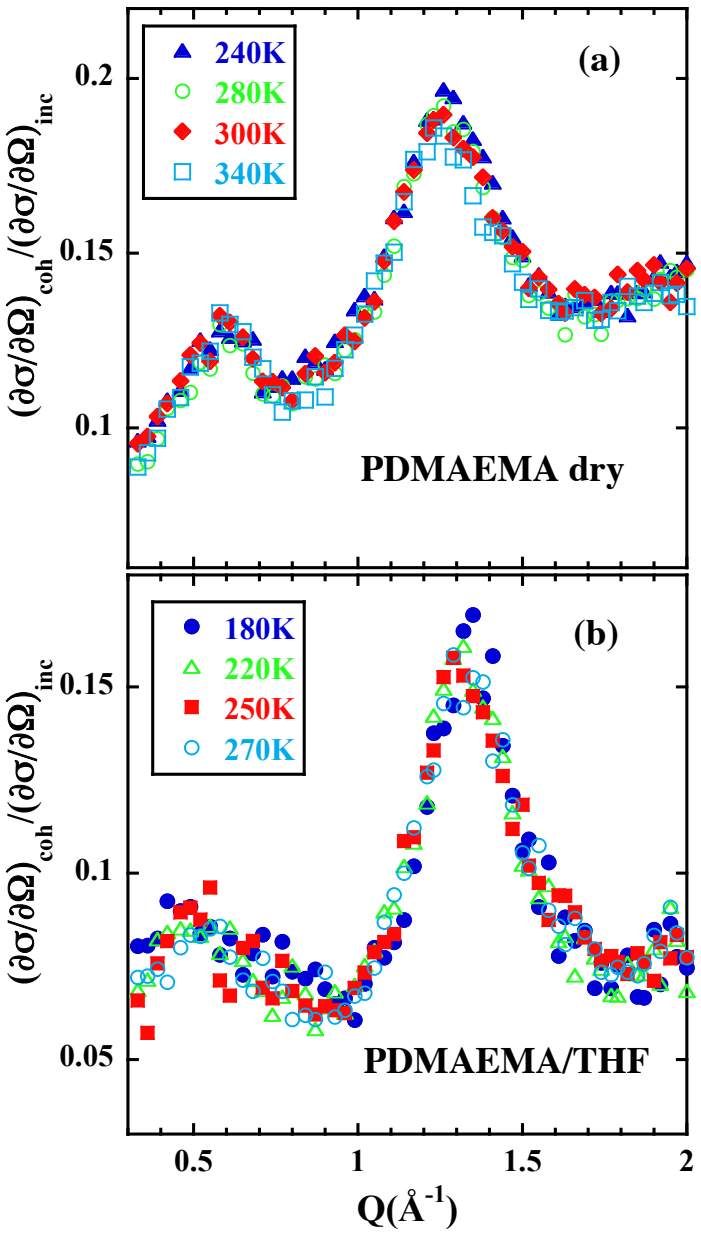

Figure 3. Ratio between coherent and incoherent differential cross sections measured by DNS at the different temperatures indicated on the dry PDMAEMA polymer (a) and on its mixture with THF (fully protonated sample) (b).

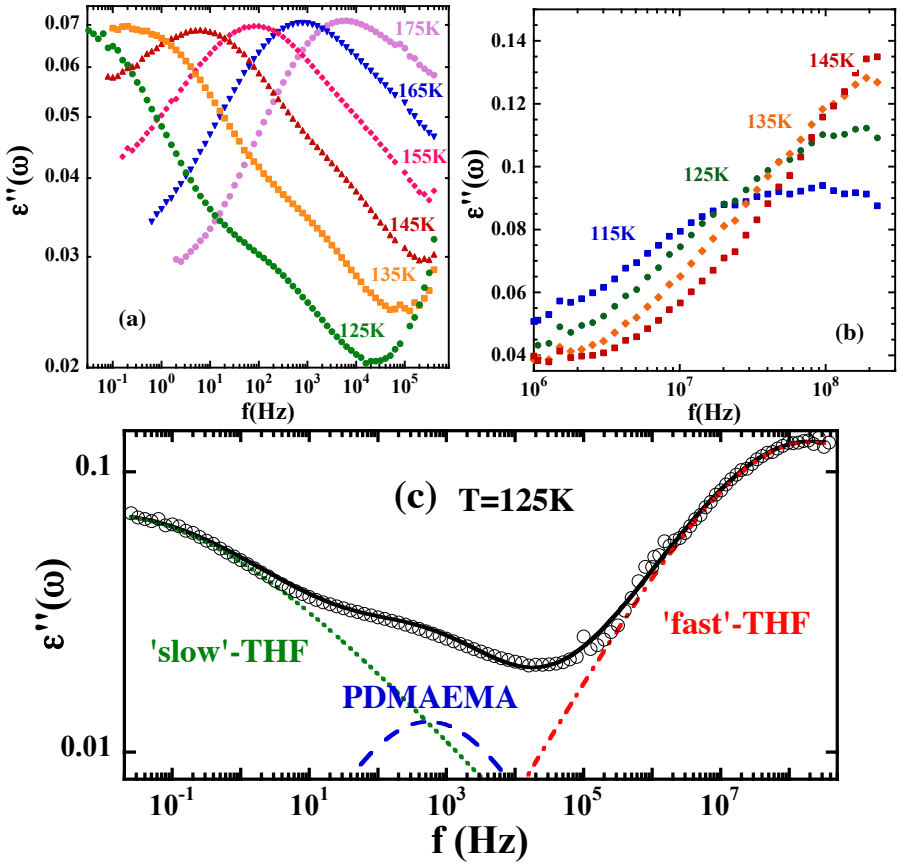

Figure 4. Dielectric loss measured on PDMAEMA/THF with the Novocontrol Alpha-S spectrometer (a) and with the Agilent E4991A RF-Impedance Analyzer (b) at the different temperatures indicated. Merged data from both instruments at 125 K are represented in (c), where solid line is the description in terms of the three Cole-Cole contributions represented by the dashed ('slow' THF-process), dotted (PDMAEMA β-relaxation) and dashed-dotted ('fast' THF-process) curves.

C. Quasielastic Neutron Scattering

For their further analysis, QENS data –acquired as function of momentum and energy transfer, i. e., of Q and $\hbar\omega$– were transformed into time domain, following a procedure which allows deconvolution from the instrumental resolution. Experimental intermediate scattering functions $S^{exp}(Q,t)$ were obtained by Fourier transforming to time domain the frequency-dependent QENS data obtained at a given temperature and Q-value. These functions were deconvoluted from the resolution function by dividing them by the corresponding $S^{exp}(Q,t)$ obtained from the spectrum measured at 10 K. Figure 5 shows as an example the such obtained final intermediate scattering functions for some representative Q-values and two different temperatures.

The incoherent fraction of the total (coherent plus incoherent) differential cross section measured by DNS on the dPDMAEMA/THF sample investigated by QENS is shown in Fig. 2. In the relevant Q-range for the QENS measurements, it amounts to about 0.75 in average. These DNS data thus confirm that the incoherent contribution largely dominates the signal for this sample. We also emphasize that this incoherent contribution is basically due to the hydrogens in the THF component: the ratio between the incoherent cross section from these nuclei and the total incoherent cross section is 0.9. The intermediate scattering functions of THF-hydrogens accessed by the QENS experiments show more pronounced decays at the higher temperature, with a tendency to reach a plateau in the long-time regime, as can be seen in Fig. 5. For a given temperature, the characteristic time for the decay does not show a clear Q-dependence. These features suggest the occurrence of spatially localized motions in the window investigated.

IV. DATA ANALYSIS AND MODELLING

A. Dielectric Spectroscopy

The processes under investigation occur in the glassy state of the system. In such situation, loss peaks usually are symmetric and describable by the imaginary part of a Cole-Cole function:

$$\epsilon^*_{CC}(\omega) = \epsilon_\infty + \frac{\Delta\epsilon}{[1+(i\omega\tau_{CC})^{\alpha_{CC}}]} \tag{3}$$

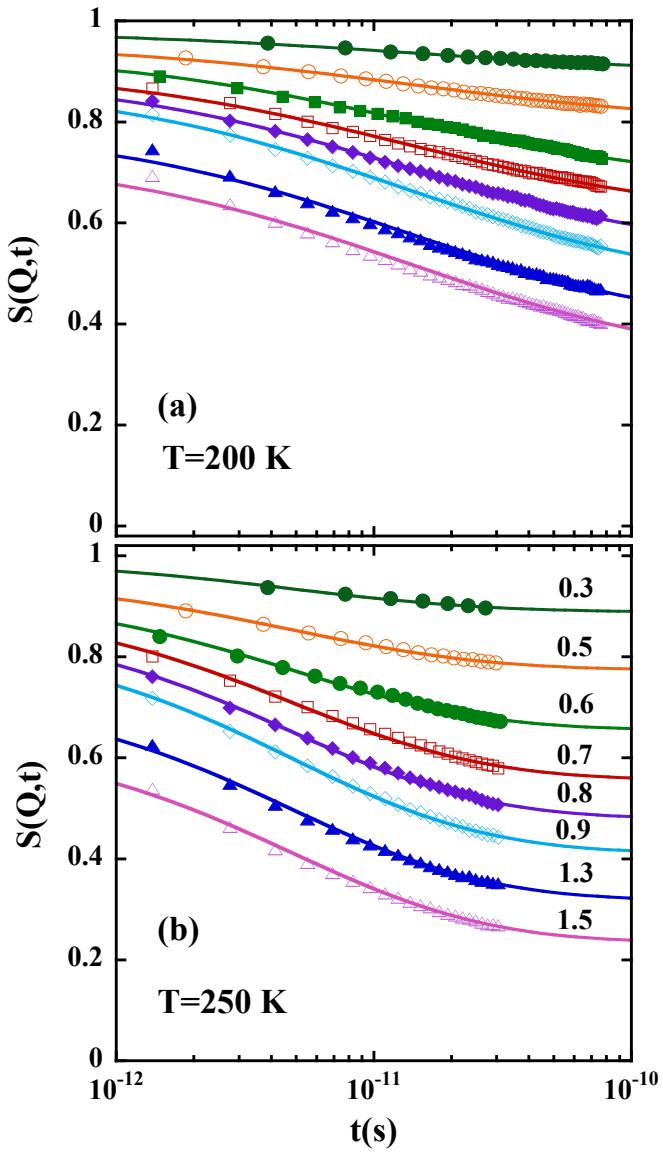

Figure 5. Intermediate scattering function of THF hydrogens in the mixture at different Q-values and $T = 200$ K (a) and $T = 250$ K (b). The Q-values are given in (b) in Å^{-1}. Data in (b) have been restricted to times shorter than 30 ps. Continues lines show the fits considering only the 'fast'-THF process with the model described in the text.

with α_{CC} the shape parameter and τ_{CC} the Cole-Cole characteristic relaxation time. This time coincides with $\tau_{max} = 1/(2\pi f_{max})$, being f_{max} the frequency of the maximum of the loss peak. As previously commented, in glassy PDMAEMA/THF three dynamical processes can be distinguished: that relevant at lower frequencies (we will call it 'slow'-THF process), a PDMAEMA relaxation contributing at intermediate frequencies and a 'fast'-THF process dominating in the high frequency range. Therefore, a combination of three Cole-Cole functions –characterized by the corresponding τ^i_{CC} and α^i_{CC} parameters, $i = s$ ('slow'-THF), $i = p$ (PDMAEMA), and $i = f$ ('fast'-THF)– was used in the fitting procedure. The quality of the fit and the resolved contributions can be seen in Fig. 4(c).

Symmetric broadenings of spectra can be attributed to the presence of distributions of relaxation times in the glassy state due to the structural disorder. For each process 'i', we may consider the relaxation times distributed according to a Gaussian function:

$$h_i[\log(\tau)] \;=\; \frac{1}{\sqrt{2\pi}\sigma_i}\exp\left(-\frac{\left[\log(\tau)-\log(\tau^i_{max})\right]^2}{2\sigma_i^2}\right) \tag{4}$$

Here, $\log(\tau^i_{max})$ determines the position of the maximum of the distribution function (which coincides with the average logarithm of the characteristic time). The width of the distribution σ_i can be calculated starting from the shape parameter α^i_{CC} of the Cole-Cole function by the empirical equation[17] :

$$\sigma_i \;=\; \frac{6.9\times10^{-4}}{{\alpha^i_{CC}}^4} - 3.8163\log(\alpha^i_{CC}) \tag{5}$$

The results obtained for the characteristic times and the width of the distributions of the three dynamical processes are represented in Fig. 6 as functions of the inverse temperature. The relaxation times follow an Arrhenius temperature dependence:

$$\tau^i_{max} = \tau^i_{\infty}\exp\left(\frac{E^i_a}{k_BT}\right) \tag{6}$$

with the parameters shown in Table I. Regarding the widths of the distributions, that corresponding to the PDMAEMA process shows a rather weak temperature dependence, in contrast to those related to the THF dynamics. In all cases, this parameter could be characterized, within the experimental uncertainties, by laws given by

$$\sigma_i = \frac{A^i_\sigma}{T} + \sigma^i_\infty \tag{7}$$

The parameters obtained are also compiled in Table I.

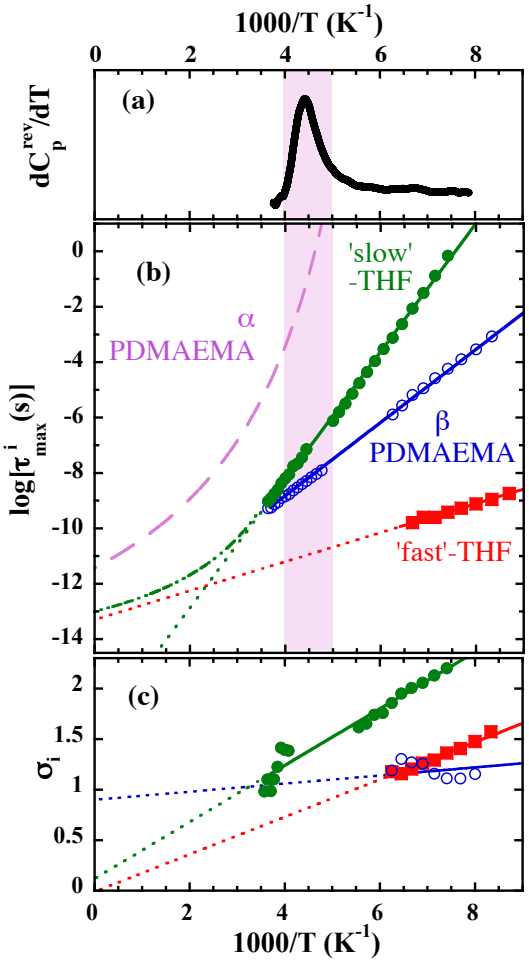

Figure 6. (a): DSC results (temperature derivative of the reversible part of the heat capacity in arbitrary units) on the PDMAEMA/THF mixture. (b) and (c): Inverse temperature dependence of the parameters characterizing the processes monitored by dielectric relaxation. (b): position of the maximum and (c): width of the distribution function of relaxation times. Filled circles correspond to the 'slow' THF-process, filled squares to the 'fast' THF-process and empty circles to PDMAEMA β-relaxation in the mixture. Lines in (b) are Arrhenius fits (eq. 6) and in (b) correspond to the law (eq. 7) with the parameters given in Table I. Dotted lines are extrapolations. In (b) the Vogel-Fulcher law describing the behavior of the α-relaxation –attributable to the polymer component– is included (dashed curve), and the dashed-dotted line depicts a suggested Vogel-Fulcher extrapolation of the 'slow' THF-process toward high temperatures. The shadowed area indicates the width of the calorimetric glass-transition.

	'fast'-THF	β-PDMAEMA	'slow'-THF
$\log[\tau^i_\infty(s)]$	-13.3 ± 0.5	-14.1 ± 0.2	-17.5 ± 0.2
E^i_a(meV)	104 ± 5	262 ± 5	459 ± 9
A^i(K)	185 ± 10	40 ± 8	280 ± 10
σ^i_∞	-0.01 ± 0.08	0.9 ± 0.1	0.12 ± 0.09

Table I. Parameters characterizing the temperature dependence of the distributions of characteristic times (position of the maximum following eq. 6 and width obeying eq. 7) of the sub-T_g processes identified in the PDMAEMA/THF mixture

B. Quasielastic Neutron Scattering

As above demonstrated, the function accessed by QENS is highly dominated by the incoherent scattering function of THF-hydrogens. QENS experiments were performed at temperatures below or slightly above the glass transition of the sample, where THF molecular motions are expected to be spatially localized. In general, the incoherent intermediate scattering function describing a localized motion is given by

$$S(Q,t) = EISF + (1 - EISF)\phi(t) \tag{8}$$

The information about the geometry of the local motion is given by the elastic incoherent structure factor (EISF), while the dynamic information (time dependence) is contained in the function $\phi(t)$. Due to the heterogeneities of the amorphous systems investigated, in the general case we expect $\phi(t)$ to result from a distribution of single exponential functions:

$$\phi(t) = \int h[\log(\tau)]\exp(-t/\tau)\mathrm{d}log(\tau) \tag{9}$$

From the DS investigation, we know that THF molecules are involved in two dynamical processes –the 'slow' and the 'fast' one–. Moreover, the DS study provided valuable and accurate information about the distributions of relaxation times underlying both relaxational processes ($h^{DS}_i(\log\tau)$, with $\log(\tau^i_{max})$ and σ_i following eqs. 6 and 7 with the parameters given in Table I). These processes take place with rather different characteristic times (see Figs. 6 and 7). Taking into account the dynamic range covered by the QENS experiments ($\approx$ 1 to

100 ps), we would expect that the 'fast'-THF process dominates the decay of the intermediate scattering function at all the temperatures investigated. However, a contribution of the 'slow'-THF process could also be expected to be appreciable at long times in the high temperature range explored (see Fig. 7). With this information at hand, we applied the following strategy to analyze the QENS results:

1. Characterization of the 'Fast'-THF Process

As argued above, the main dynamic contribution to the QENS spectra is expected to be that of the 'fast'-THF process. The corresponding intermediate scattering function $S_f(Q,t)$ can be built invoking that of a localized motion (eq. 8) with an a priori unknown $EISF = EISF_f$ and $\phi(t) = \phi_f(t)$ given by eq. 9 with the distribution function of relaxation times fixed to that determined by DS for the 'fast'-THF process $h(\log\tau) \equiv h_f^{DS}(\log\tau)$. A global pre-factor A was also included in the fitting procedure, which parametrizes the even faster contributions (motions like vibrations leading to the decay of correlations at times shorter than those accessible by the instrument). With this model, very good fits were obtained at the two lowest temperatures investigated (see representative examples for 200 K in Fig. 5(a)). At higher temperatures, this description was acceptable if the time window considered was restricted to approx. $t \leq 30$ ps (see Fig. 5(b)). The so obtained values of the $EISF_f$ parameter are depicted in Fig. 8. They decrease with increasing Q and seem to reach a saturation value of about 0.5, at least at the lowest temperatures considered. This behavior can be well described by the $EISF$ corresponding to a jump between two equivalent positions,

$$EISF_{jump} = \frac{1}{2}\left(1 + \frac{\sin(Qd)}{Qd}\right) \tag{10}$$

were d is the jump distance. The fit of eq. 10 to the obtained $EISF_f$ data delivers the characteristic jump lengths for the 'fast'-THF process d_f represented in the inset of Fig. 8. For the two lowest temperatures investigated, they are close to 3Å, while there is a tendency of this parameter to increase at higher temperatures. We remind though, that in such a temperature range QENS results could be significantly influenced by the 'slow'-THF process characterized by DS (see Fig. 7).

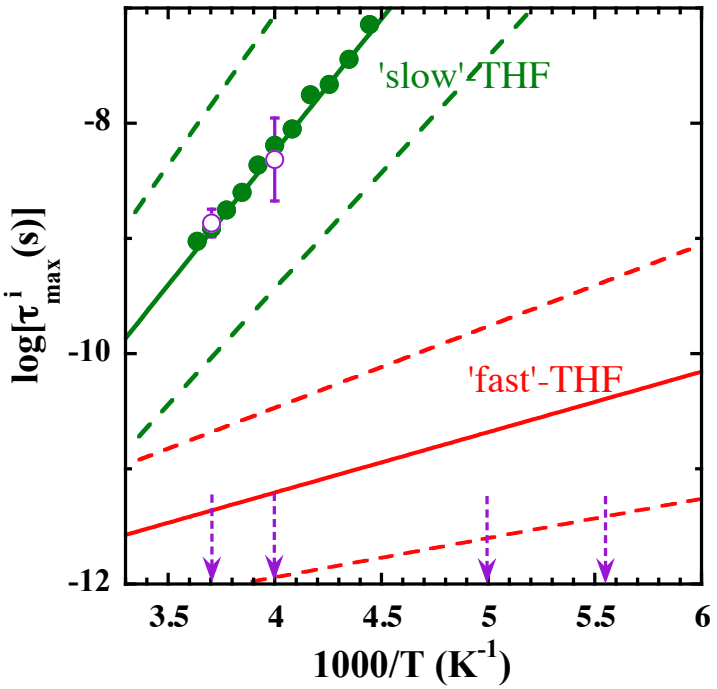

Figure 7. Magnification of the Arrhenius plot [Fig. 6(b)] in the region of interest for the QENS investigation (the location of the temperatures studied by QENS are indicated by the dotted vertical arrows). Only results referring to the THF component are represented. Solid lines are the Arrhenius fits shown in Fig. 6(b). Dashed lines represent the curves $\log \tau^i_{max} \pm \sigma_i$ delimiting the region where the distribution function of characteristic times presents the most relevant contribution. The Q-averaged results obtained for the 'slow'-THF process from the QENS investigation are included as empty circles. The error bars show their variance (see Fig. 10).

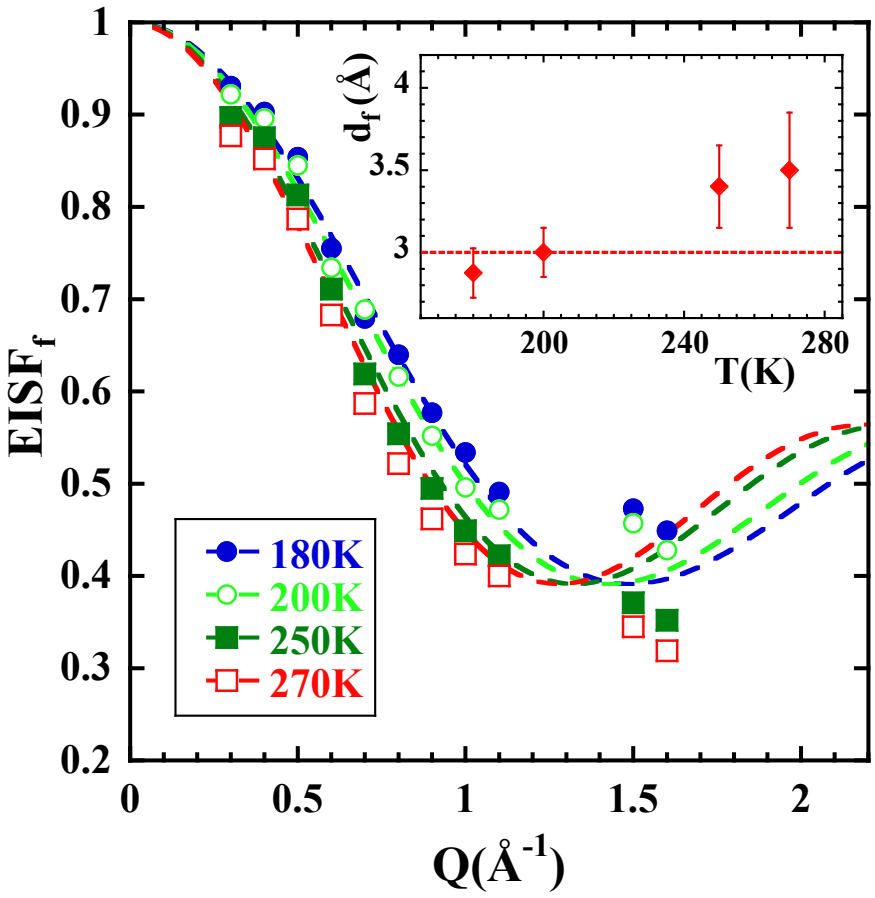

Figure 8. Wavevector dependence of the elastic incoherent structure factor corresponding to the 'fast' THF-process obtained from the analysis of the QENS results in terms of a unique contribution (and vibrations, see the text). Dashed lines are fits to the EISF corresponding to 2-sites jump. The resulting values of the jump distance d_f are represented as function of temperature in the inset.

2. Characterization of the 'Slow'-THF Process

At 250 and 270 K the 'slow'-THF process indeed contributes to the long-time decay of the intermediate scattering function. This is illustrated in Fig. 9 for the case of 250 K and $Q = 0.8$ Å^{-1}. For these conditions, the dotted line shows the intermediate scattering function corresponding only to the 'fast'-THF process (and fast vibrational contributions) obtained as described in the previous analysis step. Obviously, this curve does not describe the tendency at long times ($t \geq 30$ ps approx.) of the experimental data. We thus analyzed the high-temperature QENS results considering the occurrence of both kinds of motions, aiming to obtain additional information on the 'slow'-THF process, in particular regarding its geometry. We assumed the a priori simplest scenario: simultaneous (independent) occurrence of the localized 'fast' and 'slow' processes in THF. This translates into the following intermediate scattering function:

$$S(Q,t) = A\{[EISF_f + (1 - EISF_f)\phi_f(t)][EISF_s + (1 - EISF_s)\phi_s(t)]\} \qquad (11)$$

where the two intermediate scattering functions corresponding to each process are multiplied.

We tried to fix the maximum number of parameters in the fitting procedure. Therefore, we considered $EISF_f$ to be given by eq. 10 with a temperature independent value of $d_f = 3$ Å (that deduced in the previous step for 180 and 200 K, where QENS data are free from slower contributions), and $\phi_f(t)$ to be completely fixed to that determined from DS. For the 'slow'-THF process, we assumed for $\phi_s(t)$ a Gaussian distribution of characteristic times with the width σ_s as determined from the DS study. Thus, only three parameters were allowed to float: the overall amplitude A, the average characteristic time $\log \tau^s_{max}$ and $EISF_s$ of the 'slow'-process. From the Q-dependence of the QENS results, the most suitable functional form for the $EISF_s$ parameter was found to be that corresponding to motions lying within a sphere of radius r_s:

$$EISF_s = \frac{9}{(Qr_s)^6}\left(\sin(Qr_s) - Qr_s\cos(Qr_s)\right)^2 \qquad (12)$$

with a value of $r_s \approx 4.3$ Å. The fitting curves obtained describe very accurately the experimental intermediate scattering functions, as can be seen in Fig. 9. The values of $\log(\tau^s_{max})$ used for these descriptions are represented in Fig. 10 as function of the scattering

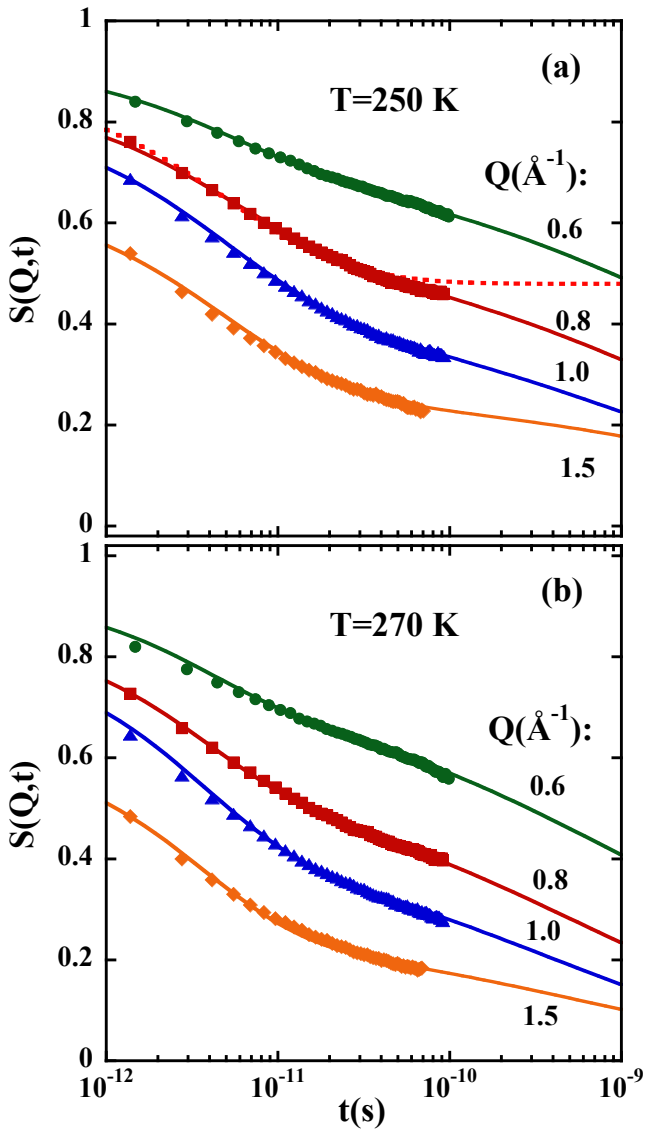

Figure 9. Intermediate scattering function of THF hydrogens in the mixture at $T = 250$ K (a) and $T = 270$ K (b) and the different Q-values indicated. Continues lines show the fits considering both, the 'fast' and the 'slow' THF process with the model described in the text (eq. 11). For $Q = 0.8$ Å^{-1}, the description obtained assuming only the 'fast' contribution is shown for comparison as a dotted line in (a).

vector and compared with the dielectric counterparts at the same temperatures. The QENS results oscillate around the values determined from DS. This behavior could be due to the presence of coherent contributions in the intermediate scattering function (note the kind of modulation with the coherent component of the scattered intensity, see Fig. 2), which are very difficult to take into account in the model function. We have calculated the Q-averaged value of this parameter as obtained from QENS, $\langle \log(\tau^s_{max}) \rangle_Q$, as well as its variance. The results are displayed in Fig. 7 (empty circles and error bars) in comparison with the dielectric results. As can be seen in this context, the effect from coherent contributions is not so important, mainly at the highest temperature investigated. We can thus state that, within the uncertainties, the same relaxation times distribution is found from both, the dielectric and the QENS studies, also for this 'slow'-THF process.

V. DISCUSSION

Knowledge about the structural features can be very useful to interpret and understand the dynamical processes. We therefore first analyze the structural information provided by scattering techniques on our system.

The patterns of the three samples investigated by DNS (Figs. 2 and 3) show a common peak at $Q = 1.3$ Å^{-1} presumably related to short-range order features. The strong increase toward low Q-values in the labelled sample dPDMAEMA/THF arises from the contrast between protonated and deuterated components in the mixture. Supporting this assessment, we observe that this small angle contribution is not present in the data collected on the sample with both components protonated (see Fig. 3(b)), where such contrast is practically absent. The overall features of the pattern of this sample resemble those of the dry sample shown in Fig. 3(a): a main peak around $Q_{II} = 1.3$ Å^{-1}, and an additional one at about $Q_I = 0.5...0.55$ Å^{-1}. This peak is obviously hidden by the strong small angle contribution in the partially deuterated sample. Diffraction patterns obtained by X-rays with better statistics also show such a clear peak (see Fig. 11) at $Q_I \approx 0.5$ Å^{-1}. The presence of this kind of 'pre-peaks' is typical for polymers with long or relatively bulky side-groups like e. g. the families of poly(n-alkyl methacrylates)[18] , poly(n-alkyl acrylates)[19] , poly(itaconates)[20] , poly(alkylene oxides)[21] , polystyrene[22] , poly(vinyl pirrolidone)[23] and some polyelectrolytes[24,25]. Based on experimental hints and aid from molecular dynamics

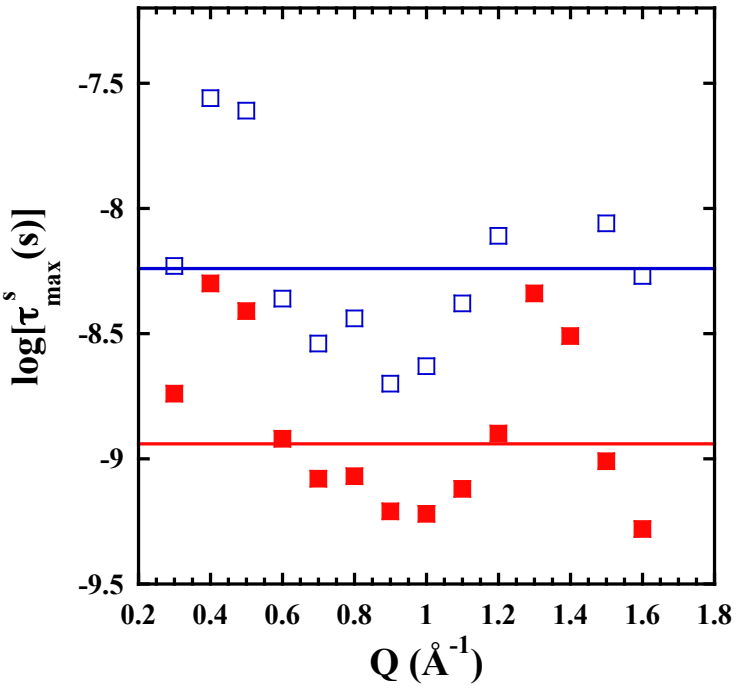

Figure 10. Wavevector dependence of the characteristic time deduced for the 'slow' THF process from the QENS investigation at 250 K (empty symbols) and 270 K (filled symbols). For 250 K, the slow contribution cannot be really resolved at 1.3 and 1.4 Å^{-1}. Horizontal lines indicate the corresponding values obtained from the dielectric study.

simulations[26], it is now established that such systems present a kind of nano-phase segregation between side groups and main chains leading to the existence of nano-domains rich in each of the polymeric subspecies. The existence of the 'pre-peak' is a consequence of this phenomenon, and from its position the size of the nano-domain D can be estimated as $D \approx 2\pi/Q_I$. For PDMAEMA thus a value of $D \approx 12$Å can be deduced. This size is not appreciably affected by the presence of THF molecules, since the peak position is hardly shifted upon addition of THF. The width of the peak is not significantly influenced either, within the uncertainties. We thus infer that the overall nano-domain structure is essentially the same in the dry polymer and in the mixture, ruling out a significant presence of clusters of solvent molecules that would distort the ordering naturally induced in the polymer by the segregation of main-chain and side-group atoms. We would thus expect that the THF molecules would be homogeneously distributed within the sample, maintaining also locally the macroscopic average concentration of one molecule per monomer.

Now moving to the results on the dynamics, we have identified two different dynamical processes in THF as minority component in a mixture with PDMAEMA. QENS qualifies both processes as localized motions taking place in a simultaneous way –i. e., as statistically independent events. Thanks to the combination of dielectric spectroscopy and QENS techniques we have been able to characterize their associated distributions of characteristic times as well as their geometrical features. It is worth emphasizing that, within the uncertainties, for both processes we have been able to describe the QENS data with the relaxation times distribution determined from the dielectric spectroscopy investigation. In the following we discuss on the nature of the two THF-processes, in view of the obtained results and in the light of other works in the literature.

Let us assume that the elementary event underlying a given observed process is a simple activated jump over a barrier E_a. Then, its jump rate $1/\tau$ obeys an Arrhenius law $1/\tau = \nu_{vib} \exp[-E_a/(k_B T)]$, with ν_{vib} the attempt frequency –which should be typically of the order of the phonon frequencies in the system, i. e., $\nu_{vib} \approx 10^{13} s^{-1}$. Let us now assume that structural disorder induces different environments leading to a distribution of barriers $g(E_a)$. In the simplest case, $g(E_a)$ is a Gaussian function

$$g(E_a) = \frac{1}{\sqrt{2\pi}\sigma_{E_a}} \exp\left(-\frac{[E_a - \langle E_a \rangle]^2}{2\sigma_{E_a}^2}\right). \tag{13}$$

The existence of this distribution is accompanied by a Gaussian distribution of the logarithm

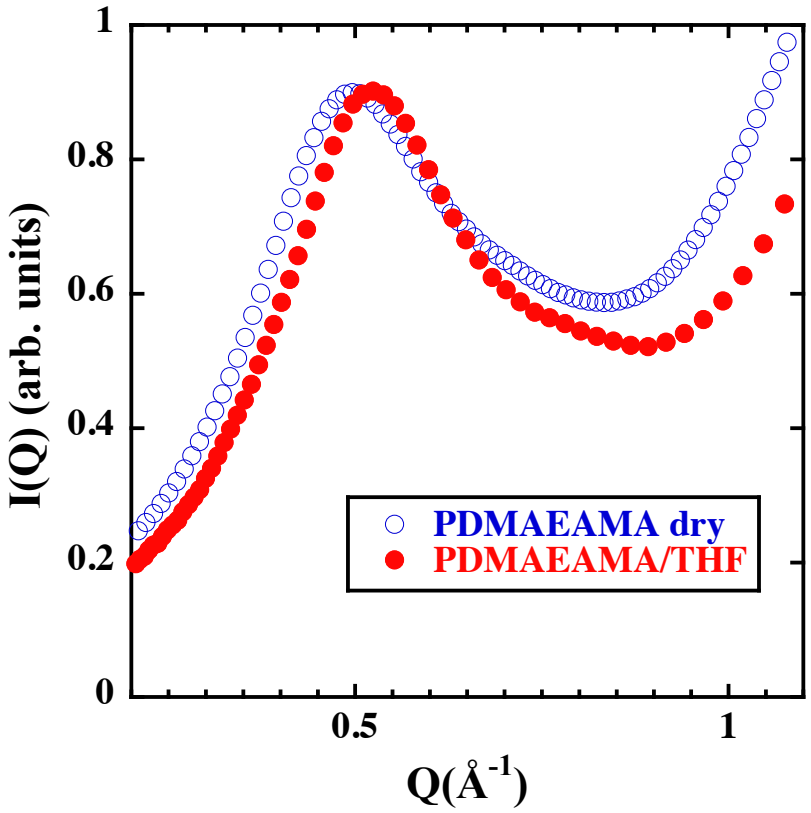

Figure 11. X-Ray diffraction patterns obtained by SAXS on the dry PDMAEMA polymer (empty symbols) and on its mixture with THF (fully protonated sample) (filled symbols) at RT. The intensities have been scaled to coincide in the maximum of the peak.

of characteristic times τ (eq. 4) where: (i) the average characteristic time displays the prefactor of the elementary process $1/\nu_{vib}$ and the average activation energy $\langle E_a \rangle$ and (ii) the width is simply given by $\sigma_{E_a} \log(e)/k_B T$. This means, if E_a is the only distributed magnitude for an ensemble of simply thermally activated processes leading to a given relaxation 'i', then: (i) τ_∞ in eq. 6 should have a meaningful value attributable to a real attempt frequency and (ii) σ^i_∞ in eq. 7 should be zero.

These two conditions are fulfilled for the 'fast'-THF process. We can thus describe this relaxation as due to activated motions with activation energies distributed according a Gaussian function centered around an average value of $\langle E^f_a \rangle = 104$ meV with a width of $\sigma^f_{E_a} = 36.5$ meV. The value of $\langle E^f_a \rangle$ is in the range of typical energy barriers corresponding to simple molecular motions like e. g. methyl-group rotations, but the width is about twice as large as that usually found for such motions in glassy polymers[27] . A possible reason could be that the environments in the mixture are more heterogeneous than in bulk polymers. It is also worth commenting that the 'fast'-THF process here reported displays the same activation energy as the so-called δ-process observed by dielectric spectroscopy by Blochowicz et al.[6] on THF as minority component in mixtures with tristyrene (THF concentrations ϕ_{THF}=10, 20 and 33%). The characteristic times of such δ-process displayed a ϕ_{THF}-independent activation energy but decreasing absolute values with decreasing ϕ_{THF}. The 'fast'-THF process in PDMAEMA would roughly coincide with the infinite dilution limit of the δ-process observed in the mixtures with tristyrene. In that work, applying ^{2}H NMR spectroscopy they found that the motions involved in the δ-process could not be directly identified with conformational transitions between two different possible configurations reported from ab initio calculations reported by Rayon and Sordo[28] . An essential ingredient to be considered in order to describe the experimental ^{2}H NMR spectra was the geometrical distortion induced by the environment in the mixtures. In this way, Blochowicz et al. identified the occurrence of large angle jumps in THF and concluded that the origin of the δ-process should be due to an internal motion of the THF ring. From the QENS study we have deduced that the motions involved in this 'fast'-process lead to apparent hydrogen jumps between two positions separated by approx. 3 Å, in agreement with large angle jumps of the THF-ring as proposed from the ^{2}H NMR study. We also note that the scenario of very well dispersed THF molecules in the polymeric matrix would explain the coincidence of the 'fast'-THF process with the $\phi_{THF} \rightarrow 0$ limit of the δ-process reported in the mixtures with tristyrene.

Now we consider the 'slow'-THF process. It does not show any hint of Vogel-Fulcher like temperature dependence of the characteristic time in the whole temperature range investigated. In addition, DSC measurements do not reveal an additional glass-transition in the covered range (see Fig. 6(a)). Both observations obviously contradict that the 'slow'-THF process is a 'conventional' α-relaxation. Furthermore, the crossover from Vogel-Fulcher to Arrhenius temperature dependence in the vicinity of the glass transition of the slower component reported for other binary mixtures (see, e. g.[3,7,14]) cannot be resolved from our experimental results. The Arrhenius behavior of the characteristic time of the 'slow'-THF process is found up to temperatures well above the glass-transition of the PDMAEMA component, where it displays as small values as some nanoseconds. The crossover, if present in our system, would have to be seek at even higher temperatures than those investigated in this work. The dashed-dotted line in Fig. 6(b) represents a speculative extrapolation of the average characteristic time of the 'slow'-THF process toward high temperatures following a Vogel-Fulcher dependence with a sensible prefactor of 10^{-13} s. To provide an experimental univocal proof such a behavior is unfortunately extremely difficult, given the high frequency/temperature region to be explored, implying probable solvent losses and merging of the process with the 'fast'-THF relaxation.

It is noteworthy that in any case the Arrhenius extrapolation of the characteristic time of the 'slow'-THF process to high temperatures becomes unrealistic: there would be a temperature above which this time would display values smaller than those of the 'fast' process or even to those corresponding to typical phonon excitations. This is due to the small prefactor of the average characteristic time $\tau^s_\infty = 3.3 \times 10^{-18}$ s, which can definitely not be attributed to an inverse attempt frequency. Such finding is traditionally interpreted as due to contributions of entropic origin to the underlying relaxation process. In the Eyring formalism, the prefactor in the Arrhenius equation would be given by $\tau_\infty = \nu^{-1}_{vib} \exp[-\Delta S/(k_B T)]$, where ΔS is the activation entropy involved in the molecular motion. In this framework, $\Delta S/k_B \approx \ln(\bar{N}!)$, where $\bar{N}$ is the average number of elementary states involved; the non-vanishing value of σ^s_∞ would represent the distribution width around this average value. Considering $\nu_{vib} \approx 10^{13} s^{-1}$, a value of about 8 is obtained for $\bar{N}$. Now let us discuss about the nature of the entities involved in this collective process.

A key result provided by QENS spatial resolution is the evidence for localization of the relaxation mechanism underlying the 'slow'-THF process. We have deduced that THF

hydrogen motions are spatially restricted within a volume of about 8.6 Å in size. This spatial extent would be in agreement with the above proposed scenario of confinement of the THF molecules within the nano-domains (most probably in a side-group rich environment) in the nano-phase segregated PDMAEMA –we remind that the size of the domains has been determined to be of about 12 Å. Moreover, we have discarded a significant presence of THF clusters in the mixture, at least for the present concentration (one THF molecule / PDMAEMA monomer). This would imply that THF molecules are practically screened from each other by the side-groups of the polymeric matrix. Thus, PDMAEMA side-groups have to be among the molecular units involved in the relaxational process leading to the 'slow'-THF process.

We propose the following scenario for the 'slow'-THF process: at very high temperatures, THF molecules should be able to relax independently from the environment, with motions occurring with characteristic times in the range of the picosecond. Upon cooling down, these motions start to couple with the surrounding environment, which is rich in polymeric side groups. Accordingly, the activation energy of the THF motion increases. This occurs until the relaxation within the nano-domain involves $\tilde{N} \approx 8$. At lower temperatures, THF molecules undergo such localized motions 'assisted' by their neighbors within the nano-domain, which provide a local relatively large mobility. As can be seen in Fig. 6(b), in this temperature region the faster relaxational β-process of the PDMAEMA component takes place. This has been characterized in our complementary QENS study[15] as a localized motion of the side group involving rotations on discs of 3 Å radius for methylene hydrogens and 1.65 Å radius for methyl-group hydrogens (see scheme of the monomer in Fig. 1). These motions of the side groups persist below the glass transition of the polymer, when the main-chain motions freeze, providing the THF molecules the needed surrounding mobility to be able to relax.

The crossover in other systems with strong dynamic asymmetry, like e. g. water in polymer matrices[14,29–31] , is observed because cooperativity effects on the structural relaxation of the fast component become progressively enhanced with decreasing temperature down to the region where the characteristic time of this relaxation reaches values of the order of microseconds. The THF motions involved in our mixture with PDMAEMA seem to not experience such a pronounced cooperativity. We may argue that in this mixture cooperativity effects arising from THF/THF interactions would be much weaker than in the bulk mate-

rial or in large enough clusters of solvent within the polymeric matrix. We could speculate that the key ingredient for developing cooperativity effects is the direct interaction between molecular units of the same kind. This is favored if there is a significant number of nearest neighbors of the same nature around a given relaxing unit of the fast component. Such a situation is realized if the fast component forms clusters, as it is the case of water molecules interacting via H-bonds. In mixtures of polymeric units, chain connectivity would naturally provide also a source of collectivity. In our system, THF molecules seem to be screened from each other by the side-groups of the polymer. The high molecular mobility associated to these side-groups would induce a kind of 'plasticization' effect on THF motions. It is worth mentioning that the important role of local polymer relaxations on the solvent dynamics was also put forward in a study of PVME aqueous solutions[32] .

Last, we mention that in the mixtures of THF and tristyrene investigated in Ref.[6] two dielectric relaxations with characteristic times longer than that of the previously commented δ process were also attributed to the THF component. For ϕ_{THF}=0.33%, the slowest one was found in a similar frequency/temperature regime as the 'slow'-THF process here reported. That process –called α'– was interpreted as the confined α-relaxation of THF molecules in the mixture, but it was characterized in a very narrow range (characteristic times between about 1 and 10^{-3} s.) due to its merging with the α-process. Thus, a crossover could not be identified. The relaxation with intermediate characteristic times between those of the so-called α' and δ is independent of THF-concentration and was identified by those authors as the β-process of the THF component. It was characterized as due to small-amplitude reorientations of the THF molecules. In our system we could not identify any THF motion of such characteristics from the QENS investigation, which is selectively sensitive to this component. In the same time/temperature region though, the dielectric response of the THF/PDMAEMA mixture presents the dynamical process that we have assigned[15] to the β-relaxation of the polymer component (see Fig. 6(b)). This identification was proved by a complementary QENS study on the PDMAEMA dynamics in this mixture, through which we robustly characterized the dielectric relaxation assigned to the PDMAEMA β-process in terms of polymeric motions that can also be found in the dry polymer. We thus conclude that the origin of such intermediate relaxation in triphenyl and in PDMAEMA mixtures with THF has to be of different nature.

VI. CONCLUSIONS

The combination of dielectric spectroscopy and neutron scattering on a labelled sample has allowed characterizing the dynamics of THF molecules in a mixture with PDMAEMA. Two independent processes have been identified. The 'fast' one has been qualified as due to an internal motion of the THF ring leading to hydrogen displacements of about 3 Å. The activation energies of this motion are rather broadly distributed around an average value of 104 meV. The 'slow' process is characterized by an Arrhenius-like temperature dependence of the characteristic time which persists in the whole range investigated, up to very high temperatures, where the times reach values in the range of some nanoseconds. The QENS results evidence the confined nature of this process, determining a size of about 8 Å for the volume within which THF hydrogens' motions are restricted. We could tentatively assign this process to the α-relaxation of THF molecules confined by the slower or even rigid polymeric matrix. However, (i) no signature of a crossover toward a cooperative character in the temperature range where the matrix is well mobile could be identified and (ii) no indications for a calorimetric glass transition could be resolved.

Valuable information about the structural properties of the mixture has been extracted from scattering experiments. The presence of a 'pre-peak' in the structure factor of the dry polymer is indicative for nano-phase separation into main-chain and side-groups domains of about 12 Å in size. Such a nano-structuring remains essentially unchanged upon addition of the THF molecules at the concentration investigated (1 THF molecule per monomer). This observation rules out a significant presence of clusters of solvent molecules, pointing to a scenario where THF molecules are well dispersed among the nano-domains of the polymer matrix and thus rather isolated from each other. More precisely, they experience an environment rich in polymeric side groups. Such a dispersion, together with a locally highly mobile environment provided by the side groups, would prevent cooperativity effects between THF molecules to develop for the structural relaxation of the solvent, frustrating there by the emergence of Vogel-Fulcher-like behavior even at very high temperatures. We thus interpret the 'slow'-THF process as a confined process involving collectivity with other few molecular units –mainly polymeric side-groups– within the nano-domains of the polymeric PDMAEMA matrix.

VII. ACKNOWLEDGEMENTS

Financial support from the Projects MAT2012-31088 and IT-654-13 (GV) is acknowledged. This work is based on experiments performed at TOFTOF and DNS (Heinz Maier-Leibnitz Zentrum (MLZ), Garching, Germany), and has been supported by the European Commission under the 7th Framework Programme through the 'Research Infrastructures' action of the 'Capacities' Programme, NMI3-II Grant Number 283883.

REFERENCES

[1]J. Colmenero and A. Arbe, Soft Matter **3**, 1474 (2007).

[2]A. Arbe, A. Alegría, J. Colmenero, S. Hoffmann, L. Willner, and D. Richter, Macromolecules **32**, 7572 (1999).

[3]C. Lorthioir, A. Alegría, and J. Colmenero, Physical Review E **68**, 031805 (2003).

[4]J. W. Sy and J. Mijovic, Macromolecules **33**, 933 (2000).

[5]S. Zhang and J. Runt, Journal of Polymer Science Part B: Polymer Physics **42**, 3405 (2004).

[6]T. Blochowicz, S. Lusceac, P. Gutfreund, S. Schramm, and B. Stuhn, The Journal of Physical Chemistry B **115**, 1623 (2011).

[7]T. Blochowicz, S. Schramm, S. Lusceac, M. Vogel, B. Stühn, P. Gutfreund, and B. Frick, Physical Review Letters **109**, 035702 (2012).

[8]A.-C. Genix, A. Arbe, F. Alvarez, J. Colmenero, L. Willner, and D. Richter, Physical Review E **72**, 031808 (2005).

[9]S. Arrese-Igor, A. Alegría, A. Moreno, and J. Colmenero, Macromolecules **44**, 3611 (2011).

[10]D. Cangialosi, A. Alegría, and J. Colmenero, The Journal of Chemical Physics **126**, 204904 (2007).

[11]M. Brodeck, F. Alvarez, J. Colmenero, and D. Richter, Macromolecules **45**, 536 (2011).

[12]M. Tyagi, A. Arbe, A. Alegría, J. Colmenero, and B. Frick, Macromolecules **40**, 4568 (2007).

[13]T. W. Smith, M. A. Abkowitz, G. C. Conway, D. J. Luca, J. M. Serpico, and G. E. Wnek, Macromolecules **29**, 5042 (1996).

[14]S. Cerveny, A. Alegría, and J. Colmenero, Physical Review E **77**, 031803 (2008).

[15]G. Goracci, A. Arbe, A. Alegría, V. García-Sakai, S. Rudic, G. Schneider, F. Juranyi, and J. Colmenero, Submitted to Macromolecules.

[16]G. Goracci and et al, In progess.

[17]This equation resulted from the CC fit of the loss-curves generated with a superposition of Debye relaxations according to eq. 4 for various σ-values in the range from 0.1 to 0.5.

[18]A. Arbe, A.-C. Genix, J. Colmenero, D. Richter, and P. Fouquet, Soft Matter **4**, 1792 (2008).

[19]M. Beiner and H. Huth, Nature Materials **2**, 595 (2003).

[20]A.-C. Genix and F. Lauprêtre, Macromolecules **38**, 2786 (2005).

[21]C. Gerstl, M. Brodeck, G. Schneider, Y. Su, J. Allgaier, A. Arbe, J. Colmenero, and D. Richter, Macromolecules **45**, 7293 (2012).

[22]I. Iradi, F. Alvarez, J. Colmenero, and A. Arbe, Physica B: Condensed Matter **350**, E881 (2004).

[23]R. Busselez, A. Arbe, F. Alvarez, J. Colmenero, and B. Frick, The Journal of Chemical Physics **134**, 054904 (2011).

[24]M.-H. Kim, C. J. Glinka, S. A. Grot, and W. G. Grot, Macromolecules **39**, 4775 (2006).

[25]C. F. Buitrago, D. S. Bolintineanu, M. E. Seitz, K. L. Opper, K. B. Wagener, M. J. Stevens, A. L. Frischknecht, and K. I. Winey, Macromolecules **48**, 1210 (2015).

[26]A. Moreno, A. Arbe, and J. Colmenero, Macromolecules **44**, 1695 (2011).

[27]J. Colmenero, A. J. Moreno, and A. Alegría, Progress in Polymer Science **30**, 1147 (2005).

[28]V. M. Rayón and J. A. Sordo, The Journal of Chemical Physics **122**, 204303 (2005).

[29]R. Busselez, A. Arbe, S. Cerveny, S. Capponi, J. Colmenero, and B. Frick, The Journal of Chemical Physics **137**, 084902 (2012).

[30]J. Swenson and S. Cerveny, Journal of Physics: Condensed Matter **27**, 033102 (2015).

[31]S. Cerveny, A. Alegría, and J. Colmenero, The Journal of Chemical Physics **128**, 044901 (2008).

[32]S. Capponi, A. Arbe, S. Cerveny, R. Busselez, B. Frick, J. Embs, and J. Colmenero, The Journal of Chemical Physics **134**, 204906 (2011).